

Mapping Global Lithospheric Mantle Pressure-Temperature Conditions by Machine-Learning Thermobarometry

Ben Qin^{1,2}, Chenyang Ye¹, Jingao Liu³, Shichun Huang⁴, Shunguo Wang⁵, J. ZhangZhou¹

1Key Laboratory of Geoscience Big Data and Deep Resource of Zhejiang Province, School of Earth Sciences, Zhejiang University, Hangzhou, China,

2School of Resource and Environmental Engineering, Inner Mongolia University of Technology, Hohhot, China,

3State Key Laboratory of Geological Processes and Mineral Resources, China University of Geoscience, Beijing, China,

4Department of Earth and Planetary Sciences, The University of Tennessee, Knoxville, TN, USA,

5Department of Electronic Systems, Norwegian University of Science and Technology, Trondheim, Norway

Introduction

The pressure-temperature (P-T) conditions of the lithospheric mantle are critical for Earth's interior processes, including magma genesis and cratonic stabilization (Lee et al., 2011). These conditions, which also define the lithosphere-asthenosphere boundary (LAB), are determined through methods like mineral thermobarometers, seismic observations, and geothermal models (Artemieva, 2009). Mantle xenoliths, sampled directly from the lithospheric mantle, help constrain these P-T conditions using thermobarometers developed from high-temperature and pressure experiments (e.g. Nimis & Taylor, 2000). However, these traditional thermobarometers often overfit and have limited application across different compositions. Recently, machine learning (ML) has emerged as a tool to handle the complexity of these correlations. This study evaluates classic thermobarometers against new ML-based models to better understand the lithospheric mantle's geotherm.

Data and Methods

Our study employed XGBoost to develop ML-based thermobarometry for predicting lithospheric mantle P-T conditions. We compiled over 985 high-temperature and high-pressure experiments and a global dataset of mantle peridotites from the GEOROC database to train the XGBoost models. Additionally, the models were used to construct a thermal LAB model, integrating geophysical observations to advance mantle dynamics analysis.

Results

We developed ten ML-based models: 4 barometers (Cpx, Opx, Cpx-Opx, and Opx-Grt) and six thermometers (Cpx, Opx, Cpx-Opx, Opx-Grt, Ol-Grt, and Ol-Sp). To assess their performance, we evaluated the R^2 values from 1,000 random training-testing splits (Figure 1). The R^2 values for barometers ranged between 0.52 to 0.94, and for thermometers between 0.30 to 0.93. We selected models representative of the peak R^2 values from these distributions for further analysis. For example, the Cpx-Opx barometer and thermometer demonstrated high accuracy, with final R^2 values of 0.84 and 0.82, respectively, on the testing sets and training-set RMSE of 0.7. Errors were estimated by averaging the absolute differences between measured and predicted values, yielding ± 0.5 GPa for the barometer and $\pm 56^\circ\text{C}$ for the thermometer. These selected models were used to predict pressures and temperatures of global xenoliths.

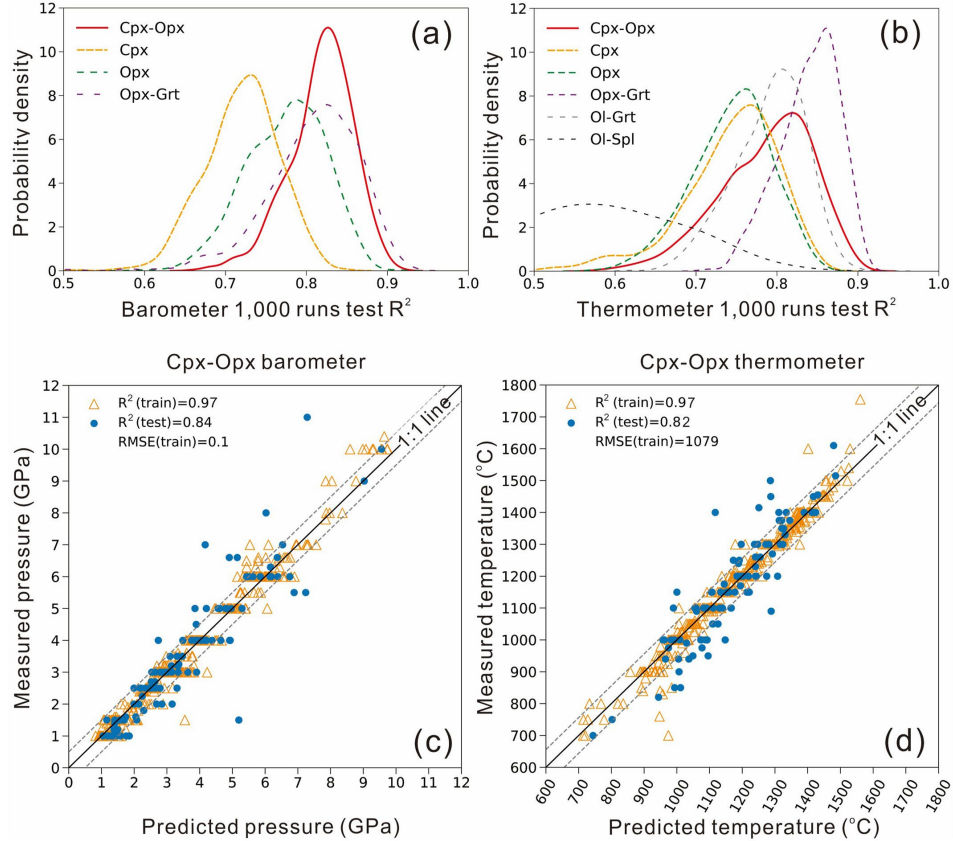


Figure 1. Machine learning model performance. (a), (b) Distributions of R^2 values obtained over 1,000 random training/testing data set splittings of the barometers and thermometers, respectively. (c), (d) Final clinopyroxene-orthopyroxene barometer and thermometer models, respectively. Dotted lines represent 1σ uncertainties which are $y = x \pm 0.5$ GPa and $y = x \pm 56^{\circ}\text{C}$ in (c) and (d), respectively.

Discussion

The ML predictions indicated cooler surface heat fluxes of $40\text{-}50\text{ mW m}^{-2}$ for the Slave, Rae, and Kalahari Cratons, with some areas of the Kalahari reaching $50\text{-}60\text{ mW m}^{-2}$, suggesting thick lithospheres (Figure 2). In contrast, the Siberian, West African, and North China Cratons displayed warmer and thinner lithospheres with heat fluxes of $60\text{-}80\text{ mW m}^{-2}$ and LAB depths of $75\text{-}125\text{ km}$ (Figure 2), reflecting significant lithospheric thinning, particularly in the North China Craton. Oceanic samples, influenced by magmatic activities and potentially contaminated by recycled material, typically surface from depths of $50\text{-}100\text{ km}$ (Figure 2). This analysis, driven by our ML thermobarometry, highlights diverse geothermal gradients and lithospheric dynamics across various cratons and oceanic regions.

Seismic waves show a 2% reduction in shear-wave velocity at the lithosphere-asthenosphere boundary (LAB), mapped using the LithoRef18 (Afonso et al., 2019) model integrated with geophysical data. Our model, calibrated with ML thermobarometer data, suggests the LAB is generally $0\text{-}80\text{ km}$ deeper in thermal models than in geophysical models due to different data sensitivities. Discrepancies arise from the thermal model detecting thermal transitions and the geophysical model responding to compositional changes. Two scenarios explain these differences: one involves a melt-bearing zone affecting seismic velocities (Wu et al., 2020) and the other suggests higher water content in the asthenosphere influences seismic properties (Hua et al., 2023). Integrating these findings offers a more comprehensive understanding of the LAB's complex dynamics.

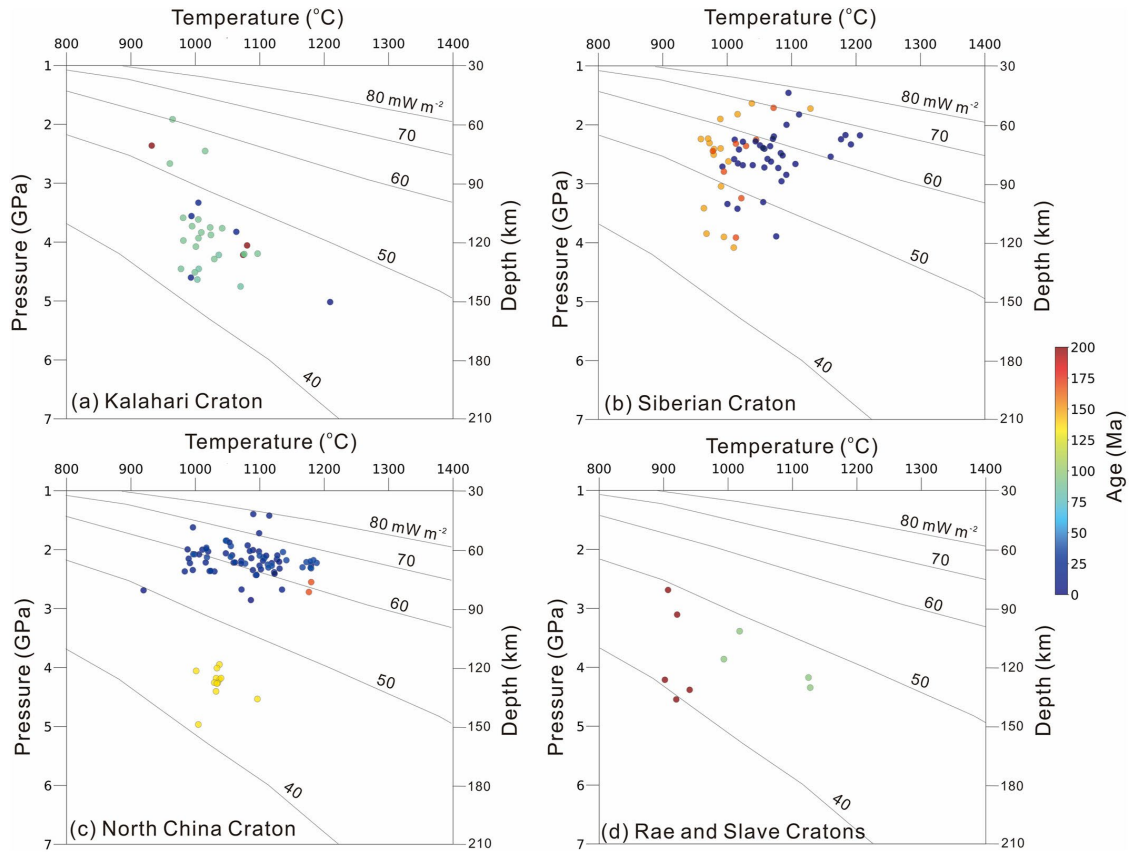


Figure 2. Temporal variations in equilibrium P-T conditions across cratons, indicated by host magma eruption ages: (a) Kalahari, (b) Siberian, (c) North China, (d) Rae and Slave Cratons. Symbols colored by eruptive ages.

References

- Afonso JC, Salajegheh F, Szwillus W, Ebbing J, Gaina C (2019) A global reference model of the lithosphere and upper mantle from joint inversion and analysis of multiple data sets. *Geophys J Int*, 217:1602–1628.
- Artemieva, I. M (2009) The continental lithosphere: Reconciling thermal, seismic, and petrologic data. *Lithos* 109:23–46.
- Chen, T., Guestrin, C. (2016). XGBoost: A scalable tree boosting system. In *Proceedings of the 22nd ACM SIGKDD international conference on knowledge discovery and data mining* (pp. 785–794).
- Hua J, Fischer KM, Becker TW, Gazel E, Hirth G (2023) Asthenospheric low-velocity zone consistent with globally prevalent partial melting. *Nat Geosci* 16:175–181.
- Lee CTA, Luffi P, Chin EJ (2011) Building and destroying continental mantle. *Annu Rev Earth Planet Sci* 39:59–90.
- Nimis P, Taylor WR (2000) Single clinopyroxene thermobarometry for garnet peridotites. Part I. Calibration and testing of a Cr-in-Cpx barometer and an enstatite-in-Cpx thermometer. *Contrib Mineral Petrol* 139:541–554.
- Wu Z, Chen L, Talebian M, Wang X, Jiang M, Ai Y (2021). Lateral structural variation of the lithosphere-asthenosphere system in the northeastern to eastern Iranian plateau and its tectonic implications. *J Geophys Res Solid Earth* 126:e2020JB020256.